Optical Phase Locking techniques: an overview and a novel method based on Single Side Sub-Carrier modulation

Optical Phase Locking techniques: an overview and a novel method based on Single Side Sub-Carrier modulation

V. Ferrero[1*] and S. Camatel[2]

[1]*PhotonLab, Dipartimento di Elettronica, Politecnico di Torino, C.so Duca degli Abruzzi 24, 10129 Torino, Italy.*
[2]*PhotonLab, Istituto Superiore Mario Boella, Via P. C. Boggio 61, 10138 Torino, Italy*
**Corresponding author: valter.ferrero@polito.it*

Abstract: A short overview on Optical Phase locking techniques and a detailed description of the Phase Locking technique based on Sub-Carriers modulation is presented. Furthermore, a novel Single Side Sub-Carrier-based Optical Phase Locked Loop (SS-SC-OPLL), with off the shelf optical components, is also presented and experimentally demonstrated. Our new method, based on continuous wave semiconductor lasers and optical single side sub-carrier modulation using QPSK $LiNbO_3$ modulator, allows a practical implementation with better performance with respect to the previously proposed OPLL circuits, and permits an easy use in real time WDM signal coherent demodulation.

OCIS codes: (060.1660) Coherent communications, (060.2920) Homodyning, (060.5060) Phase Modulation, (060.2360) Fiber optics links and subsystem, (060.4510) Optical Communications

References and links

1. L. G. Kazovsky, "Balanced phase-locked loops for optical homodyne receivers: performance analysis, design considerations, and laser linewidth requirements," J. Lightwave Technol. **4**, 182-195 (1986).
2. E. Bonek, W. R. Leeb, A. L. Scholtz, and H. K. Phillipp, "Optical PLLs see the light," Microwaves & RF **22**, 65-70 (1983).
3. A. L. Scholtz, W. R. Leeb, H. K. Philipp, and E. Bonek, "Infra-red homodyne receiver with acousto-optically controlled local oscillator," Electron. Lett. **19**, 234-235 (1983).
4. D. J. Malyon, T. G. Hodgkinson, D. W. Smith, R. C. Booth, and B. E. Daymond-John, "PSK homodyne receiver sensitivity measurements at 1.5 μm," Electron. Lett. **19**, 144-146 (1983).
5. G. L. Abbas, V. W. S. Chan, and T. K. Lee, "Local oscillator excess noise suppression for homodyne and heterodyne detection," Opt. Lett. **8**, 419-421 (1983).
6. D. J. Malyon, "Digital fibre transmission using optical homodyne detection," Electron. Lett. **20**, 281-283 (1984).
7. D. J. Malyon, D. W. Smith, and R. Wyatt, "Semiconductor laser homodyne optical phase-locked-loop," Electron. Lett. **22**, 421-422 (1986).
8. L. G. Kazovsky, and D. A. Atlas, "A 1320-nm experimental optical phase-locked loop: performance investigation and PSK homodyne experiments at 140 Mb/s and 2 Gb/s," J. Lightwave Technol. **8**, 1414-1425 (1990).
9. J. M. Kahn, B. L. Kasper, and K. J. Pollock, "Optical Phaselock receiver with multigigahertz signal bandwidth," Electron. Lett. **25**, 626-628 (1989).
10. H. K. Philipp, A. L. Scholtz, E. Bonek, and W. R. Leeb, "Costas loop experiments for a 10.6 um communications receiver," IEEE Trans. Commun. **31**, 1000-1002 (1983).
11. L. G. Kazovsky, "Decision-driven phase-locked loop for optical homodyne receivers: performance analysis and laser linewidth requirements," J. Lightwave Technol. **3**, 1238-1247 (1985).
12. S. Norimatsu, K. Iwashita, and K. Sato, "PSK Optical Homodyne Detection Using External Cavity Laser Diodes in Costas Loop," IEEE Photon. Technol. Lett. **2**, 374-376 (1990).
13. T. G. Hodgkinson, "Costas loop analysis for coherent optical receivers," Electron. Lett. **22**, 394-396 (1986).
14. Y. Wang, and W. R. Leeb, "Costas loop self-homodyne experiment for a diode laser receiver," Electron. Lett. **22**, 686-687 (1986).
15. S. Norimatsu, K. Iwashita, and K. Noguchi, "10Gbit/s optical PSK homodyne transmission experiments using external cavity DFB LDs," Electron. Lett. **26**, 648-649 (1990).

#86423 - $15.00 USD Received 13 Aug 2007; revised 12 Nov 2007; accepted 12 Nov 2007; published 9 Jan 2008

16. S. Norimatsu, K. Iwashita, and K. Noguchi, "An 8 Gbit/s QPSK Optical Homodyne Detection Experiment Using External-Cavity Laser Diodes," IEEE Photon. Technol. Lett. **4**, 765-767 (1992).
17. J. R. Barry, and J. M. Kahn, "Carrier Synchronization for Homodyne and Heterodyne Detection of Optical Quadriphase-Shift Keying," J. Lightwave Technol. **10**, 1939-1951 (1992).
18. L. H. Enloe, and J. L. Rodda, "Laser Phase Locked Loop," Proc. IEEE **53**, 165-166 (1965).
19. W. R. Leeb, H. K. Philipp, A. L. Scholtz, and E. Bonek, "Frequency synchronization and phase locking of CO_2 lasers," Appl. Phys. Lett. **41**, 592-594 (1982).
20. J. M. Kahn, "1 Gbit/s PSK homodyne transmission system using phase-locked semiconductor lasers," IEEE Photon. Technol. Lett. **1**, 340-342 (1989).
21. G. Fischer, "A 700 Mbit/s PSK Optical Homodyne System with Balanced Phase Locked Loop," J. Opt. Commun. **9**, 27-28 (1988).
22. T. J. Kane, and E. A. P. Cheng, "Fast frequency tuning and phase locking of diode-pumped Nd:YAG ring lasers," Opt. Lett. **13**, 970-972 (1988).
23. S. Norimatsu, H. Mawatari, Y. Yoshikuni, O. Ishida, and K. Iwashita, "10Gbit/s optical BPSK homodyne detection experiment with solitary DFB laser diodes," Electron. Lett. **31**, 125-127 (1995).
24. S. Camatel, V. Ferrero, R. Gaudino, and P. Poggiolini, "Optical phase-locked loop for coherent detection optical receiver," Electron. Lett. **40**, 384-385 (2004).
25. V. Ferrero, S. Camatel, R. Gaudino, and P. Poggiolini, "A novel Optical Phase Locked Loop architecture based on Sub-Carrier modulation," in *Proceedings Optical Fiber Communication Conference*(Optical Society of America, Washington, DC, United States, 2004), pp. 615-617.
26. S. Camatel, and V. Ferrero, "Homodyne coherent detection of ASK and PSK signals performed by a subcarrier optical phase-locked loop," IEEE Photon. Technol. Lett. **18**, 142-144 (2006).
27. S. Norimatsu, and K. Iwashita, "PLL propagation delay-time influence on linewidth requirements of optical PSK homodyne detection," J. Lightwave Technol. **9**, 1367-1375 (1991).
28. S. Camatel, and V. Ferrero, "2.5-gb/s BPSK ultradense WDM homodyne coherent detection using a subcarrier-based optical phase-locked loop," IEEE Photon. Technol. Lett. **18**, 1919-1921 (2006).
29. L. G. Kazovsky, "Phase- and Polarization-Diversity Coherent Optical Techniques," J. Lightwave Technol. **7**, 279-292 (1989).

1. Introduction

Optical Phase Locking techniques for coherent detection, received great attention at the beginning of the 90s [1-22] in order to increase the receiver sensitivity, but they never found practical applications, firstly because of their complexity, secondly due to the introduction of EDFAs, that greatly leveraged sensitivity issues. In the near future, anyway, coherent detection may come again of age in some of the following scenarios: Multilevel optical phase modulation (N-PSK), dispersion compensation in the electrical domain, ultra-dense WDM, fast reconfigurable optical networks, optical sensors, microwave photonics, etc.

In this paper we present a short overview on Optical Phase locking techniques in section 2, a focused analysis on Sub-Carrier Optical Phase Locked Loop technique (SC-OPLL) in section 3, and a novel Single Side Sub-Carrier-based Optical Phase Locked Loop (SS-SC-OPLL) in section 4. In section 5 we show the experimental results obtained with both techniques, the SC-OPLL and the novel SS-SC-OPLL, and in section 6 the discussion on the experimental results follows. Finally, in section 7 the conclusion.

2. Phase-locking techniques

The fundamental Optical Phase Locked Loop (OPLL) configuration is shown in Fig. 1. The proposed architecture is based on three basic elements: the phase detector, the loop filter and the optical voltage controlled oscillator (OVCO).

The phase detector combines the optical received (RX) and the local oscillator (LO) signals and it returns the electrical signal proportional to the phase error.

#86423 - $15.00 USD Received 13 Aug 2007; revised 12 Nov 2007; accepted 12 Nov 2007; published 9 Jan 2008

Many phase detector types were presented in the past and determined the OPLL architecture. Note that Fig. 1 represents also the homodyne receiver fundamental configuration block scheme. In this case the phase detector output is proportional to the phase error and the detected data signals. A first OPLL classification can be made separating linear and non-linear OPLLs. In a linear OPLL useful for PSK demodulation, inside the phase detector the RX and the LO signals are combined by a 3 dB directional coupler, and the resulting optical signal is converted in the electrical domain by one photodiode (single branch loop) or two balanced photodiodes (balanced loop). By this way the phase detector operation is performed. In order to use linear OPLL like PSK homodyne receiver, proper phase locking operations have to be guaranteed. For this reason, the transmitted signal containing the PSK data must include also a residual carrier, so the LO locks in quadrature to it, and, as a result, in phase to the data signal [1]. The residual carrier can be practically achieved by incomplete phase modulation (i.e., using a phase shift lower than 180˚). The simplest linear OPLL is a single branch OPLL [2] and early homodyne experiments were conducted implementing this configuration [3, 4]. The described phase detector is employed for the demonstration of our locking techniques based on sub-carrier modulation, presented in the following sections. The best linear OPLL is the balanced OPLL, which were originally proposed in [5], and later used in many homodyne detection experiments [6-9]. It includes two photodiodes that are interconnected so that, the signal difference between their photocurrents, drives the following transimpedance amplifier (TIA). This solution presents several advantages: it utilizes the optical power signal from both coupler output ports, and it tends to cancel the DC currents associated with the RX and the LO signals power. This approach permits to have a coherent optical receiver less sensitive to the local oscillator optical power fluctuations.

In a non-linear loop, no residual carrier is employed, so the overall RX signal optical power is useful for coherent demodulation operations. With respect to the linear-OPLL phase detector, the RX and the LO signals are combined by a 90° hybrid instead of 3 dB coupler, so the hybrid returns the in-phase combination on one output port, and the in-quadrature combination on the other output port [10, 11]. The in-phase combination output signal is converted into an electrical data signal by a photodetector or a couple of balanced photodetector; such a signal is proportional to the transmitted data. The in-quadrature combination output signal is converted into an electrical phase-lock signal by a photodetector or a couple of balanced photodetectors, and must be non-linearly processed in order to be used for phase locking operations. Two kinds of processing procedures are usually employed:

* The phase-lock signal is multiplied by the data signal; this approach is used in Costas loops architecture [10, 12-14].
* The phase-lock signal is multiplied by the recovered data; this approach is used in decision-driven loops architecture [11, 15].

Furthermore non-linear phase detector can be employed in the realization of quadrature phase shift keying (QPSK) coherent receivers [16, 17].

The loop filter is the element that has to be correctly configured in order to have a properly working loop. Many publications, focused on loop filter design and its parameters settings, are present in the literature [1, 11], so this argument will not be discussed in this paper.

The last element to take in consideration is the optical voltage controlled oscillator (OVCO), which is fundamental for the realization of an OPLL. It should generate an optical continuous wave (CW) signal whose frequency is controlled by an input voltage. Many LO

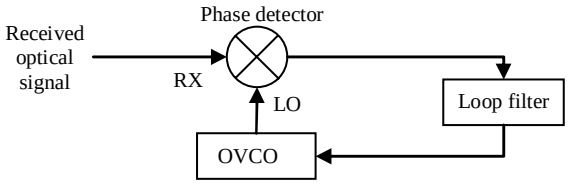

Fig. 1. Block diagram of an optical phase-locked loop.

#86423 - $15.00 USD Received 13 Aug 2007; revised 12 Nov 2007; accepted 12 Nov 2007; published 9 Jan 2008

were proposed in the past and an overall summary of the employed techniques follows:

- At the beginning, the OPLLs [18] employed, as LO, an HeNe external cavity laser in which one of the mirrors was mounted on a piezoelectric mechanical transducer, useful for phase cavity tunability. Due to the limited piezoelectric transducer time response, the OPLL employing this OVCO presented some problems to lock the RX signal frequency.
- CO2 lasers worked as LO in [2, 3, 19] where slow frequency tuning is obtained by mounting one of the resonator mirrors on a piezoelectric element. Also in this case, such first control was too slow to follow fast frequency changes and an additional frequency control mechanism based on an acousto-optic modulator was implemented.
- An external cavity semiconductor laser (ECL) was used as LO in [7]; a LiNbO3 phase modulator was placed inside the cavity in order to obtain frequency modulation. First homodyne detection using ECLs was reported in [20] where frequency modulation is obtained by directly driving the two-electrode chip, corresponding to the anode and the cathode of the ECL laser.
- The use of an acousto-optic modulator was re-proposed in [21] as an external modulator driven by an electrical VCO for tuning the frequency of a CW HeNe gas laser. The main disadvantage of the acousto-optical single-sideband modulation is the dead time on the order of 1 μs.
- Diode pumped Nd:YAG lasers were employed as LO in [8, 22]; frequency tuning was realized by installing a thin plate of piezoelectric material on the resonator. Such a slow tuning was fast enough for phase locking thanks to the excellent stability and narrow linewidth of the Nd:YAG lasers used.
- Multi-electrode DFB lasers were examined in [23]; with respect to a single-electrode DFB, multi-electrode DFB lasers respond to a frequency modulation with a reduced phase rotation. The phase rotation was proved to be limited to 36°, which is a small enough value for the OPLL stability.
- The use of semiconductor laser with sub-carrier modulation for locking operations, have been proposed from the authors of this paper in [24]. The detailed explanation is presented in the follow sections.

3. The sub carrier optical phase locked loop technique

In this section, we analyze the Sub-Carrier Optical Phase Locked Loop Technique (SC-OPLL). The architecture is based on external modulation of a CW laser; the only requirement imposed to the optical source is that intensity and phase noises must be opportunely limited in order to guarantee good phase-locking performance. The great advantage of this technique with respect to the other ones described in the previous section is that frequency modulation does not introduce undesired phenomena such as spurious phase rotation or spurious amplitude modulation. Furthermore frequency tuning is as fast as tuning the electrical VCO included in the SC-OPLL, so high bandwidth OPLLs can be realized. In this technique, frequency tuning is obtained through optical Sub-Carrier (SC) generation and tuning, and will be indicated as SC-OPLL [24-26].

#86423 - $15.00 USD Received 13 Aug 2007; revised 12 Nov 2007; accepted 12 Nov 2007; published 9 Jan 2008

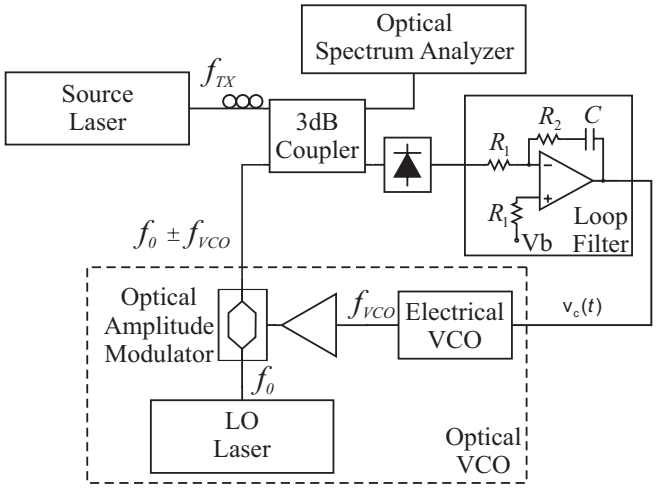

Fig. 2. Schematic of the Sub-Carrier Optical Phase Locked Loop architecture.

3.1 SC-OPLL architecture

The SC-OPLL architecture is shown in Fig. 2. The Optical Voltage Controlled Oscillator (OVCO) is the key-element and is based on a commercial Continuous-Wave (CW) external cavity tunable laser at frequency f_0, that is externally amplitude modulated by the signal coming from an electrical VCO at frequency f_{VCO}. By biasing the external Mach-Zehnder (MZ) optical amplitude modulator at a null of its transfer function, a sinusoidal carrier-suppressed modulation is obtained. The resulting spectrum at the OVCO output is shown in

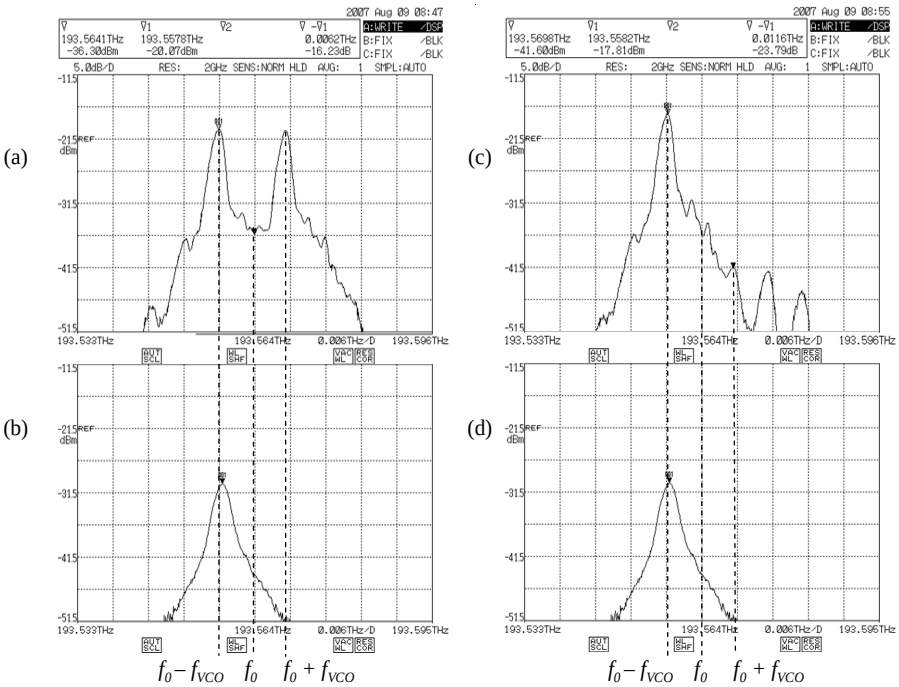

Fig. 3. SC-OPLL OVCO output (a) and RX signal (b) optical spectra when the two signals are phase-locked. SS-SC-OPLL OVCO output (c) and RX signal (d) optical spectra. Resolution Bandwidth: 0.01 nm.

#86423 - $15.00 USD Received 13 Aug 2007; revised 12 Nov 2007; accepted 12 Nov 2007; published 9 Jan 2008

Fig. 3(a). Two main SCs at frequency $f_0 \pm f_{VCO}$ are generated, with spurious optical tones at f_0 and $f_0 \pm 2 \cdot f_{VCO}$. Using one of the two main SCs, for example the one at $f_0 - f_{VCO}$, we are able to tune an *optical* frequency by simply changing the voltage applied to the *electrical* VCO, thus implementing an OVCO. Actually, this is the key issue of the proposed architecture, that allows *optical* fine frequency tuning with the speed and stability of an *electrical* VCO, and thus to re-use typical RF PLL set-ups. In our case, a standard second-order PLL control circuit allows to lock $f_0 - f_{VCO}$ to the transmitted signal at frequency f_{TX} (laser A in Fig. 2). When the OPLL is locked to $f_0 - f_{VCO} = f_{TX}$, optical homodyne is obtained, allowing to track the incoming optical signal frequency and phase.

When the incoming signal is modulated, its optical spectrum is translated to base-band at the photodiode output. In principle, due to beating with the other SCs, copies of this signal appears also around frequencies f_{VCO} and $2 \cdot f_{VCO}$, but they can be filtered out by the receiver filter, provided that f_{VCO} is larger than the signal spectral width (or bandwidth). Other set-up details can be found in Fig. 2. An active polarization controller matches the polarization of TX and LO signals before being combined by a 3dB coupler and sent to an amplified photodiode. The resulting electrical signal is processed by a single-pole active filter, in order to obtain a second-order PLL with natural frequency f_0 and damping factor ξ [1], which both depend on the loop filter parameters $\tau_1 = R_1 C$ and $\tau_2 = R_2 C$.

3.2 SC-OPLL experimental set-up

The SC-OPLL architecture of Fig. 2 was implemented using two C-band commercial external cavity tunable lasers (having a declared linewidth smaller than 700 KHz), an electrical VCO with 100 MHz/V tuning coefficient and 6.2 GHz central frequency, and a 10 GHz $LiNbO_3$ optical amplitude modulator. Fig. 3(a) shows the spectrum measured at the OVCO output, while Fig. 3(b) shows the spectrum emitted by the ECL A of Fig. 2. We obtained coarse (and slow) optical frequency tuning by changing the external cavity CW frequency, while fine (and fast) frequency tuning (i.e. phase locking operations) was obtained through our SC-OPLL principle.

4. The single side sub-carrier optical phase locked loop technique

In this section, we analyze the Single Side Sub-Carrier Optical Phase Locked Loop Technique (SS-SC-OPLL). This is a novel phase locking technique based on the use of sub-carrier modulation for frequency tuning, but with respect to SC-OPLL, in the SS-SC-OPLL only one sub-carrier is generated, so spurious beats are completely eliminated in the coherent demodulation operations. The architecture is based, like SC-OPLL, on commercial off-the-shelf optoelectronic components and without the use of gas laser or solid state laser and without *fast* direct laser frequency tuning.

4.1 SS-SC-OPLL architecture

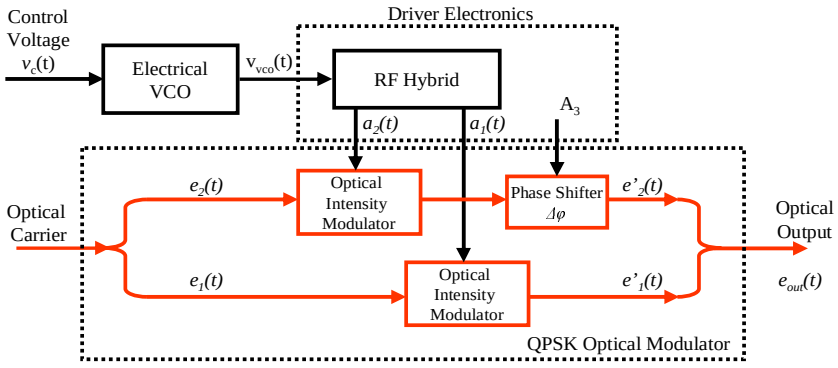

Fig. 4. Block diagram of the Optical Voltage Controlled Oscillator used in the Single Side Sub Carrier Optical Phase Locked Loop.

#86423 - $15.00 USD Received 13 Aug 2007; revised 12 Nov 2007; accepted 12 Nov 2007; published 9 Jan 2008

The SS-SC-OPLL is based on a new concept of OVCO. The new OVCO is shown in Fig. 4; it includes an RF hybrid and a particular realization scheme of a QPSK modulator made by Avanex. This particular QPSK modulator is composed by two arms, where the optical carrier is modulated by two Mach-Zehnder intensity modulators (one for each arm). A phase shifter guarantees a fixed phase difference between the two optical signals in the two arms output.

In order to explain the OVCO operation principle, the analytic signal notation is used to describe mathematically the optical signals present in the two QPSK modulator arms:

$$e_1(t) = e_2(t) = A_0 \cdot e^{j2\pi f_0 t} \tag{1}$$

The driving electrical signals applied to the two Mach-Zehnder modulators are given by:

$$\begin{aligned} a_1(t) &= k_1 \cos(2\pi f_{VCO} t + \varphi_1) \\ a_2(t) &= k_2 \cos(2\pi f_{VCO} t + \varphi_2) \end{aligned} \tag{2}$$

Where f_O is the optical carrier frequency in input to the optical QPSK modulator, and f_{VCO} is the frequency of the electrical VCO output signal $v_{VCO}(t)$.

The electrical device "RF Hybrid" is chosen in order to verify the following conditions:

$$\begin{aligned} k_1 &= k_2 = k \\ \varphi_2 &= \varphi_1 - \frac{\pi}{2} \end{aligned} \tag{3}$$

In order to simplify the following analysis, the intensity modulators and the phase shifter are assumed to be linear with an infinite extinction ratio. The effects of the non-linearity and the limited extinction ratio will be discussed later. Thus, the resulting optical signal at the QPSK modulator output is given by:

$$e_{out}(t) = \frac{1}{\sqrt{2}}\left[e_1'(t) + e_2'(t)\right] = A_0 \cdot k\left[\cos(2\pi f_{VCO} t + \varphi_1) - \sin(2\pi f_{VCO} t + \varphi_1) \cdot e^{j\Delta\varphi}\right] \cdot e^{j2\pi f t} \tag{4}$$

where $\Delta\varphi$ is the phase shift introduced by the phase shifter. Setting the phase shift $\Delta\varphi = \pi/2$ Eq. (4) becomes:

$$e_{out}(t) = A_0 \cdot k\left[\cos(2\pi f_{VCO} t + \varphi_1) - j\sin(2\pi f_{VCO} t + \varphi_1)\right] \cdot e^{j2\pi f t} = A_0 \cdot k \cdot e^{j\left[2\pi(f - f_{VCO})t - \varphi_1\right]} \tag{5}$$

If f_{VCO} is considered constant, the resulting signal $e_{out}(t)$ is a CW optical signal, whose frequency $f'_0 = f_0 - f_{VCO}$, as shown in Fig. 3(c). Since the electrical VCO frequency is controlled by the electrical input $v_c(t)$, the resulting *optical* frequency can be tuned by changing the voltage applied to the *electrical* VCO, thus implementing an OVCO. Actually, this is the key issue of the proposed architecture, which allows *optical* fine frequency tuning with the speed and stability of an *electrical* VCO.

Comparing the single-sideband modulation with respect to the double-sideband modulation, supposing to have the same optical power on the LO spectral component used for the demodulation operations, it is important to note that in the double-sideband we have twice shot noise contribution with respect to the other case.

4.2 SS-SC-OPLL experimental set-up

The SS-SC-OPLL architecture was implemented reusing the most of the components used for the SC-OPLL of Fig. 2. The only differences consist on the OVCO shown in Fig. 4, which includes an Avanex 20 GHz $LiNbO_3$ QPSK modulator and a 90° RF hybrid. The electrical VCO is the same used for the SC-OPLL realization. Fig. 3(c) shows the spectrum measured at the OVCO output, which still includes spurious spectral lines at frequencies f_0, $f_0 + f_{VCO}$ and $f_0 \pm 2f_{VCO}$. Such tones are due to the components non-ideality characteristics; in particular the residual carrier still exists due to a non infinite extinction ratio, while the suppressed sub-

#86423 - $15.00 USD Received 13 Aug 2007; revised 12 Nov 2007; accepted 12 Nov 2007; published 9 Jan 2008

carrier at frequency $f_0 + f_{VCO}$ can not be completely eliminated because we were not able to perfectly balance the signals in the two optical QPSK modulator arms. Furthermore the spectral lines $f_0 \pm 2f_{VCO}$ are generated by the power drivers characteristic non-linearity, drivers placed after the RF hybrid in order to amplify the electrical signals applied to the QPSK modulator RF inputs. With our set-up, each spurious spectral line power level is at least 20 dB lower than the LO spectral component $f_0 - f_{VCO}$, as shown in Fig. 3(c). Such a suppression showed to be adequate in order to make the SS-SC-OPLL work properly.

SS-SC-OPLL allows coarse (and slow) optical frequency tuning, by changing the external cavity CW frequency, and fine (and fast) frequency tuning (i.e., phase locking operations) through its principle.

5. Experimental results on SC-OPLL and SS-SC-OPLL techniques

In order to demonstrate the performance of ours SC-OPLL and SS-SC-OPLL, we implemented both architectures of Fig. 2 and Fig. 4, as described in the previous sections. Using the phase error estimation technique described in [8], we measured the root-mean square (RMS) OPLL phase error when locked to a CW optical signal. The OPLL phase error can be measured vs. the OPLL natural frequency f_n (which can be varied by changing the loop filter parameters while keeping ξ=0.7). For both OPLLs, the minimum phase error obtained by the described procedure is around 5 degree RMS, and was obtained for f_n slightly higher than 3 MHz, as shown in Fig. 5 [24]. We verified by numerical simulation that the OPLL had a phase error close to the theoretical one, which is limited only by the intrinsic linewidth of the used optical sources. A 5-degree RMS phase error is perfectly acceptable for coherent transmission. For instance, it gives a penalty lower than 0.1 dB in a BPSK system [1].

Note that the RMS phase error is both lasers linewidth and propagation loop time dependent; indeed appropriate values, in the design stage, have to be chosen in order to have RMS phase error lower than 5-degree, for addition information see [1, 11, 27].

In order to further check systems performance, we ran a BPSK 2.5 Gbps transmission experiment with single-branch pilot carrier receiver based on SC-OPLL and SS-SC-OPLL, where the set-up is shown in Fig. 6. The transmitter includes an external cavity tunable laser with the same LO laser characteristics. In order to transmit a residual carrier, an NRZ signal of 3.3 Vpp was applied to the phase modulator, which requires $V\pi$ = 5 V in order to produce a 180˚ phase shift. Such a configuration generates a BPSK signal with ±59.4˚ modulation angle, by leaving a residual carrier containing almost 26 percent of the transmitted power.

The Amplified Spontaneous Emission (ASE) noise and the Variable Optical Attenuator (VOA) add a variable amount of optical noise to the transmitted optical signal, useful for

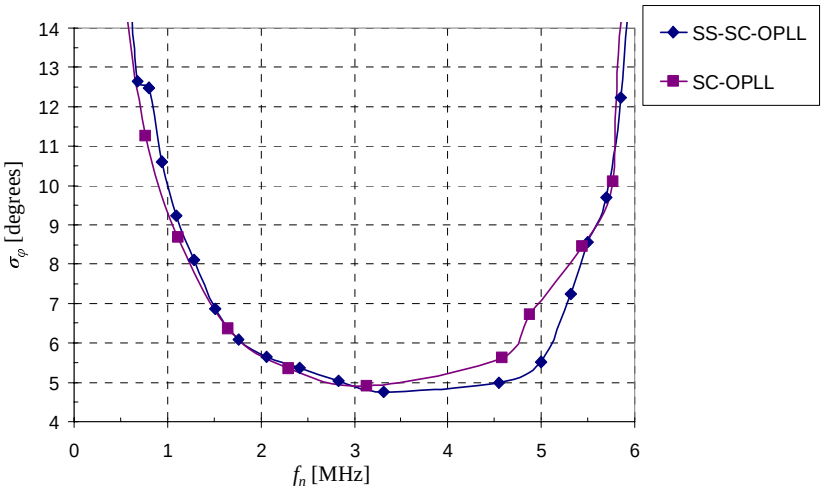

Fig. 5. Measured phase error standard deviation versus OPLL natural frequency for Sub-Carrier and Single Side Sub-Carrier Optical Phase Locked Loops.

#86423 - $15.00 USD Received 13 Aug 2007; revised 12 Nov 2007; accepted 12 Nov 2007; published 9 Jan 2008

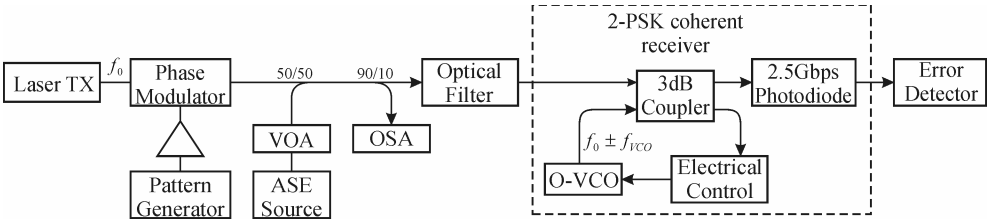

Fig. 6. Experimental set-up, for Sub-Carrier and Single Side Sub-Carrier Optical Phase Locked Loop demonstrations.

performance characterization. This configuration allows changing the Optical Signal to Noise Ratio (OSNR), measured by an Optical Spectrum Analyzer (OSA) with a resolution bandwidth of 0.1 nm, and it also allows keeping the received signal power constant to -12 dBm at the coherent optical receiver input.

The resulting BER, as a function of the received signal OSNR (defined over 0.1 nm bandwidth), is shown in Fig. 7.

6. Discussion on SC-OPLL and SS-SC-OPLL experimental results

The analyzed SC-OPLL technique shows advantages in terms of simple realization set-up and on terms of using "off the shelf" optical components. The disadvantages of this technique are due to the use of only one of the two main sub-carriers as optical local oscillator ($f_0 - f_{VCO}$), so the other one remaining ($f_0 + f_{VCO}$) is a local oscillator spurious spectral component with the same power of the used one ($f_0 - f_{VCO}$), as shown in Fig. 3(a). This local oscillator spurious spectral component introduces penalty in the coherent receiver operations, indeed only one main sub-carrier is used, so only half of the overall local oscillator power is employed.

The novel SS-SC-OPLL technique maintains the SC-OPLL advantages described above, besides it is not affected by the SC-OPLL local oscillator spurious spectral component ($f_0 + f_{VCO}$), as shown in Fig. 3(c). Therefore, in the SS-SC-OPLL case, the overall LO optical power can be used for coherent demodulation and the beat between the optical noise and the spurious spectral component is eliminated, so SS-SC-OPLL presents approximately 3 dB better performance with respect to the SC-OPLL technique, as shown in Fig. 7. Note that in our experiments, the performance is limited by ASE noise and the shot noise contribution generated in the two cases is different, but negligible in both cases.

About the SC-OPLL technique, the presence of the local oscillator spurious spectral

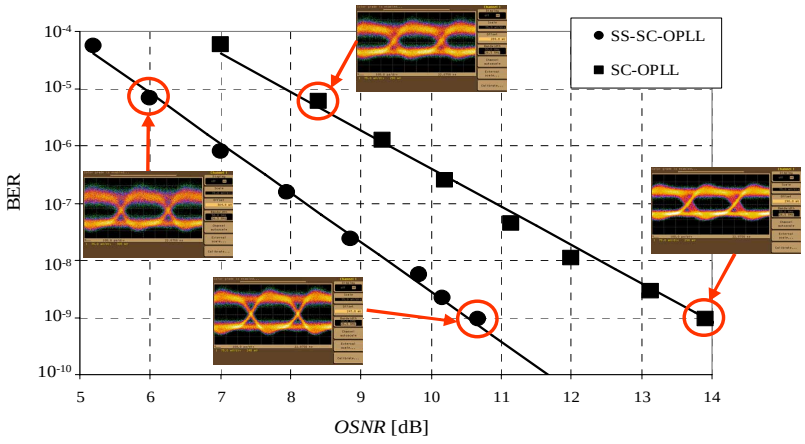

Fig. 7. BPSK 2.5 Gbps transmission experiment: measured BER versus the OSNR (Resolution Bandwidth 0.1 nm) for SS-SC-OPLL and SC-OPLL.

#86423 - $15.00 USD Received 13 Aug 2007; revised 12 Nov 2007; accepted 12 Nov 2007; published 9 Jan 2008

component ($f_0 + f_{VCO}$) shown in Fig. 3(a), limits the use of this receiver in WDM applications. Indeed, the local oscillator spurious spectral component introduces spurious beats between the received signal and the local oscillator, so if a WDM signal is used, some spurious beats may be present in the base-band where I expect to have only the channel to be demodulated. In order to use this technique for WDM applications, it is necessary to eliminate the in base-band spurious beats, filtering out the local oscillator spurious spectral component ($f_0 + f_{VCO}$). It can be obtained with very large spacing in frequency between the two sub-carriers (i.e. 40 GHz) and optical filtering. Note that very large spacing in frequency between the two sub-carriers means the use of an electrical VCO with very high central frequency (i.e. 40 GHz) [28], obtaining more complex and expensive OVCO.

The novel SS-SC-OPLL technique, eliminates completely the spurious beats because the local oscillator has no the spurious spectral component ($f_0 + f_{VCO}$), as shown in Fig. 3(c). For this reason, it could be employed using an electrical VCO with low central frequency (i.e. f_{VCO} = 1 GHz is enough to demodulate 2PSK @ 10 Gbps signal) and an optical QPSK modulator with modulation bandwidth approximately equal to the electrical VCO central frequency. Therefore the novel SS-SC-OPLL technique, with respect to the SC-OPLL one, permits the development of less complex and less expensive OVCO.

The theoretical limit for a SS-SC-OPLL based 2.5 Gbps BPSK System is OSNR =5.5 dB. So there is a 5 dB penalty in the realized coherent optical receiver. The causes of such a penalty are: pilot carrier method does not allow using the overall received optical power for data detection (1.3 dB penalty); LO carrier is not completely suppressed (0.4 dB penalty); the pilot carrier method is pattern dependent (1.3 dB penalty); we use a manual polarization controller for the experiment, so residual polarization misalignments may occur (1 dB penalty); finally the overall electrical filtering is not matched to the transmitted data pulse shape (1 dB penalty).

In order to reduce the overall penalty, it is possible to use a decision driven scheme at the receiver side, eliminating the pattern dependency and so avoiding the residual carrier at the transmitter side. Furthermore, it is possible to reduce the electrical filtering penalty by using optimized electrical filter (in the experiment we used naked optical receiver without any additional post-detection electrical filter). Finally, in order to reduce the penalty due to the residual polarization misalignment, it is possible to use automatic polarization controllers or a polarization-diversity optical receiver scheme [29].

Indeed, the coherent optical receiver based on SC-OPLL or SS-SC-OPLL, may be also realized in a polarization–diversity scheme; the new architecture avoids the use of the polarization controller in input to the optical receiver, but increase the optical receiver complexity because it is necessary to use two identical optical receiver in order to demodulate the two polarizations.

7. Conclusion

We presented a short overview on Optical Phase locking techniques and a detailed description of the ones based on sub-carriers modulation. In particular, a novel Single Side Sub-Carrier-based Optical Phase Locked Loop (SS-SC-OPLL) has been presented and experimentally demonstrated. The novel SS-SC-OPLL technique, like the SC-OPLL technique, does not introduce undesired phenomena such as spurious phase rotation or spurious amplitude modulation and shows advantages in terms of simple realization set-up and on terms of using "off the shelf" optical components. Furthermore, the novel SS-SC-OPLL technique, with respect to SC-OPLL, presents approximately 3 dB better performance and could be also used in WDM applications using an electrical VCO with much lower central frequency (i.e. f_{VCO} = 1 GHz is enough to demodulate 2PSK @ 10 Gbps signal), and an optical QPSK modulator with modulation bandwidth approximately equal to the electrical VCO central frequency. Therefore the novel SS-SC-OPLL technique, with respect to the SC-OPLL one, permits the development of less complex and less expensive coherent sub-systems, like OPLLs or coherent optical receivers.

#86423 - $15.00 USD Received 13 Aug 2007; revised 12 Nov 2007; accepted 12 Nov 2007; published 9 Jan 2008

Acknowledgements

Authors would like to thank Mr. E. Torrengo for his help and Avanex for its invaluable support to the experiments. This work was supported by Italian Ministry of University and Research (MIUR), STORiCo Project PRIN 2005 and partially supported by the EU FP6 Network of Excellence e-Photon/One, WP5 and WP10.

#86423 - $15.00 USD Received 13 Aug 2007; revised 12 Nov 2007; accepted 12 Nov 2007; published 9 Jan 2008